SCIENCE CHINA
Technological Sciences

• Article •

May 2016 Vol.59 No.5: 714–720
doi: 10.1007/s11431-016-6039-9

The mobility improvement of organic thin film transistors by introducing ZnO-nanrods as an zctive layer

XIE Tao, XIE GuangZhong*, DU HongFei, YE ZongBiao, SU YuanJie & CHEN YuYan

School of Optoelectronic Information, State Key Laboratory of Electronic Thin Films and Integrated Devices, University of Electronic Science and Technology of China (UESTC), Chengdu 610054, China

Received September 28, 2015; accepted December 17, 2015

Organic thin film transistors (OTFTs) based on poly(3-hexylthiophene) (P3HT)/Zinc oxide (ZnO) nanorods composite films as the active layers were prepared by spray-coating process. The OTFTs with P3HT/ZnO-nanorods composite films owned higher carriers mobility than the OTFT based on pure P3HT. It can be found that the mobility of OTFTs increased by 135% due to ZnO-nanorods doping. This was attributed to the improvement of the P3HT crystallinity and the optimization of polymer chains orientation. Meanwhile, because of the distinction of work function between P3HT and ZnO, the majority carriers would accumulate on either side of the P3HT-ZnO interface which benefited carrier transfer. The influence on the mobility of composite film was studied. In addition, the threshold voltage of devices changed positively with the increase of ZnO-nanorods due to the decrease of electrostatic potential for P3HT/ZnO-nanorods composite films. The effect could be explained by the energy level theory of semiconductor.

P3HT, ZnO-nanorods, composite film, OTFT

Citation: Xie T, Xie G Z, Du H F, et al. The mobility improvement of organic thin film transistors by introducing ZnO-nanrods as an active layer. Sci China Tech Sci, 2016, 59: 714–720, doi: 10.1007/s11431-016-6039-9

1 Introduction

New physical properties of the composites and various applications in devices is generated because of the expected synergy between the organic and inorganic components. Therefore, organic-inorganic nanocomposites have been widely applied in organic devices including photovoltaic devices [1–4], solar cells [5–8], organic thin film transistors (OTFTs) [9–11]. OTFTs are promising candidates for practical applications such as organic light-emitting diode (OLED) displays[12], radiofrequency identification (RFID) tags[13], and chemical sensors [14, 15] due to their scalability, low cost, and mechanical flexibility. Most researches on transistors based on organic-inorganic nanocomposites as active layers focused on the change of carrier mobility because carrier mobility was a dominated factor for the performance of device. Usually, organic semiconductors exhibit much lower carrier mobility than their inorganic counterparts, which hinders their applications in transistors. The potential of poly(3-hexylthiophene) (P3HT) for practical use in OTFTs is attribute to the outstanding semiconductor performance and solubility in a variety of organic solvents. In addition, the composites of P3HT and inorganic nano materials, such as, Al_2O_3, ZnO, or TiO_2 that were utilized in organic electronic devices have also been reported [6, 8, 16–20]. Mixing some distinctive materials into P3HT may deteriorate the crystallinity and introduce more localized energy states in the polymer film, which will induce the degradation of charge carrier mobility [9, 21]. However, blending the distinctive materials could improve the per-

*Corresponding author (email: gzxie@uestc.edu.cn)

formance of OTFTs in some case. For example, the composite films of conjugated polymer P3HT and TiO_2 nanorods modified with pyridine were improved the mobility[9]. Transistors based on P3HT/functionalized carbon nanotube hybrid were fabricated. It was found that the remarkable increase of the field-effect mobility was due to the high conductivity of the CNTs, which acted as conducting bridges for connecting the crystals in the P3HT film [10].

Here, the P3HT film and P3HT/ZnO-nanorods composite films were fabricated by spray-coating as active layers of OTFTs. The effects on the electrical characteristics of the OTFTs were studied. Moreover, the improvements in electrical properties of transistors with active layer thickness were discussed.

2 Experimental

2.1 Preparation of ZnO nanorods

0.073 g of cetyltrimethylammonium bromide (CTAB) and 1.92 g of sodium hydroxide (NaOH) (purchased from J&K Scientific) were added into 20 mL of distilled water to form a transparent solution. Then, Zinc nitrate hexahydrate ($Zn(NO_3)_2{\cdot}6H_2O$) (2.32 g) was dissolved into 20 mL of distilled water. The above two kinds of solution were mixed with equate volume under continuous stirring. After 70 min magnetically stirring, the prepared solution was transferred to a Teflon-lined stainless steel autoclave, and heated at 90°C for 15 h. The obtained white solid powder was separated from the solution by centrifugation, washed with distilled water and absolute ethanol for several times, respectively, and dried in air at 80°C.

2.2 OTFTs fabrication

Processes of OTFT fabrication are in agreement with our previous work [22]. The interdigital electrodes of the source and drain with channel length 25 μm and channel width 4000 μm were realized by photolithography, as shown in Figure 1(a). P3HT was dissolved in 6:1 chlorobenzene: 1, 2, 3, 4-tetrahydronaphthalene with concentration of 3mg/mL. ZnO nanorods with varying weights were added in the solutions under magnetically stirring for 1 h. Samples were fixed on a 85°C hotplate while the solution was sprayed onto the substrates. The prepared devices were heated in a vacuum drying oven at 70°C all night to remove the organic solvent. The schematic and imagine of OTFT were given by Figure 1(b) and (c), respectively. In this work, eight OTFTs with different spray-coating conditions were fabricated. The parameters of OTFTs were listed in Table 1. The current-voltage characteristics of the prepared devices were obtained by a Keithley 4200 semiconductor characterization system at room temperature (298 K) in the dry air.

3 Results and discussion

3.1 Characterization of prepared ZnO nanorods

The crystal phase of the as-prepared ZnO was characterized by XRD as shown in Figure 2. The ZnO-nanorods powder was crystalline and no further heat treatment was required. All the peaks matche well with Bragg reflections of the standard hexagonal wurtzite ZnO structure (JCPDS card no. 36-1451 as shown as the inset of Figure 2), in which no characteristic peaks for other impurities such as Zn or $Zn(OH)_2$ in the XRD patterns were observed, indicating the generation of ZnO from aqueous solution containing $Zn(NO_3)_2$ and NaOH through a simple hydrothermal treatment and no calcination process was needed. The detailed chemical mechanism was explained by Wang et al. [23]

3.2 Electrical properties of OTFTs

The electrical properties of OTFTs were related to the surface morphology of active layer. A field emission scanning

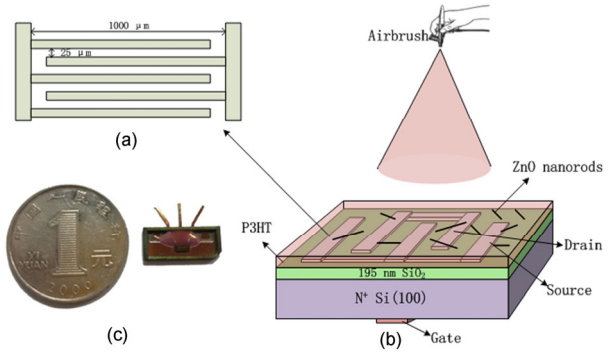

Figure 1 (Color online) Schematics of (a) interdigital electrodes of the source and drain, (b) OTFT and spray-coating process,(c) OTFT device compared to a 1 RMB coin.

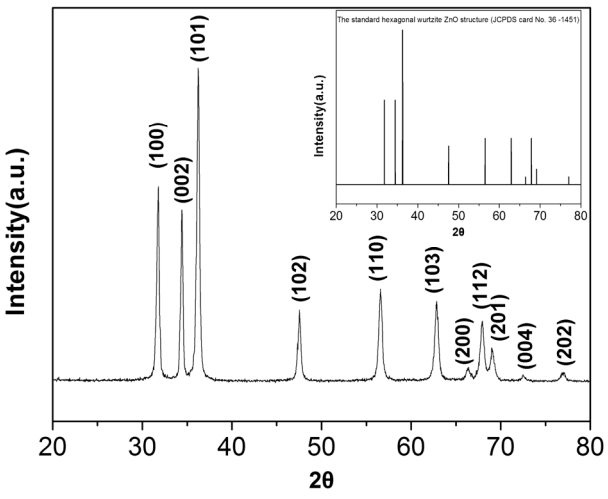

Figure 2 XRD pattern of the prepared ZnO nanorods.

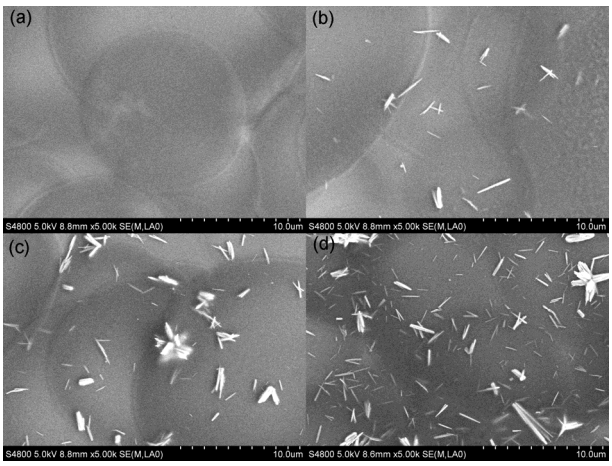

Figure 3 SEM micrographs of P3HT film with different amount of P3HT/ZnO-nanorods (a) pristine P3HT, (b) P3HT:ZnO=6:1, (c) P3HT:ZnO=6:2, (d) P3HT:ZnO=6:6.

electron microscope (FESEM, S-4800, HITACHI, Japan) operated at an acceleration voltage of 5 kV were carried out to illustrate the top surfaces of the composite films. Figure 3 illustrates SEM images of the P3HT thin films and P3HT/ZnO nanorods thin composite films. The pristine P3HT film is featureless (Figure 3(a)). Due to the spray-coating technology, there are some circles traces can be observed on the surface of film. Moreover, the P3HT/ZnO-nanorods films ascribed inhomogeneous to the aggregation of ZnO-nanorods at high ZnO-nanorods concentrations. But the aggregation condition of ZnO-nanorods dispersed in the P3HT can be improved at low concentrations.

Typical output characteristics of OTFTs at different gate bias voltages operating in the accumulation mode (gate negatively biased) were showed in Figure 4. The gate bias voltage swept from 0 V to −50 V in a step of −10 V. The dependence of I_{ds} on V_{ds} was described by Eq. (1) and Eq. (2) in linear and saturation regions, respectively. Figure 5 were transfer characteristic curves ($I_{ds}^{1/2}$ *vs* V_{gs}) of the OTFTs at V_{ds} =−50 V. The characteristic parameters of eight devices were listed in Table 1.

$$I_{ds} = \frac{WC_i\mu}{L}\left[\left(V_{gs} - V_{th}\right)V_{ds} - \frac{1}{2}V_{ds}^2\right], \quad (1)$$

$$I_{ds} = \frac{WC_i\mu}{2L}\left(V_{gs} - V_{th}\right)^2, \quad (2)$$

$$C_i = \frac{\varepsilon_i\varepsilon_0}{d}. \quad (3)$$

W and L are the channel width and length, C_i is the capacitance of the insulator, μ is carrier mobility, and V_{th} is the threshold voltage that accounts for any voltage drop at the insulator semiconductor interface and the bulk conductivity of the semiconductor layer. C_i was given by Eq. (3). d is the thickness of insulator layer, ε_i is dielectric constant of SiO_2 insulator layer and equals to 3.9. ε_0 is vacuum permittivity and equales to 8.85×10^{-14} F/cm.

The OTFTs owned a p-type semiconductor behavior, where the I_{ds} increased and then saturated with V_{ds}. Threshold voltage was the intersection of the line with the X axis, as shown in the Figure 5. Mobility values (μ) in the saturation region can be calculated using Eq. (2). The on/off currents I_{on} and I_{off} were defined as the drain-source intensity of current in the presence or in the absence of a given grain voltage, so I_{off} and I_{on} were the currents when V_{gs}= 0 V and V_{gs}= −50 V (V_{ds}= −50 V), respectively. The electrical properties of OTFTs such as V_{th}, μ and I_{on}/I_{off} were calculated and listed in Table 1.

3.3 The influence of thickness on the electronic characteristics of OTFTs

The thickness of the film was measured by profiler (Ambios XP-300). The thickness of the films was about 150 nm and 90 nm for the spray volume of 1 mL and 0.5 mL, respectively. The I_{ds} increased with the film thickness, and the similar tendency that was previously reported [24]. The variations of mobility and V_{th} as the amount of ZnO-nanorads were exhibited in Figure 6. It can be found that the mobility and V_{th} were proportional to the thickness of active film in OTFTs. For long channel devices, the surface potential may play a more important role [25]. The higher surface potential at the interface of P3HT/SiO_2 for thicker films enhanced the adsorption of holes on interface to form the channel at the same V_{gs} [26]. Therefore, the devices exhibited a more positive V_{th}. The reason of higher I_{ds} for thicker

Table 1 Parameters of OTFTs

	Sensitive film	Quantity(mL)	V_{th}(V)	I_{on}/I_{off}	μ (cm^2/Vs)
Device 1	Pure P3HT	0.5	-20.8	87.2	5.49×10^{-4}
Device 2	Pure P3HT	1	-12.8	59.8	1.30×10^{-3}
Device 3	P3HT:ZnO=6:1	0.5	-20	122.2	9.49×10^{-4}
Device 4	P3HT:ZnO=6:1	1	-10.1	26.2	1.61×10^{-3}
Device 5	P3HT:ZnO=6:2	0.5	-18.7	150.9	1.20×10^{-3}
Device 6	P3HT:ZnO=6:2	1	-7	42.9	1.83×10^{-3}
Device 7	P3HT:ZnO=6:6	0.5	-10.9	100.4	1.29×10^{-3}
Device 8	P3HT:ZnO=6:6	1	-6.1	47.6	2.62×10^{-3}

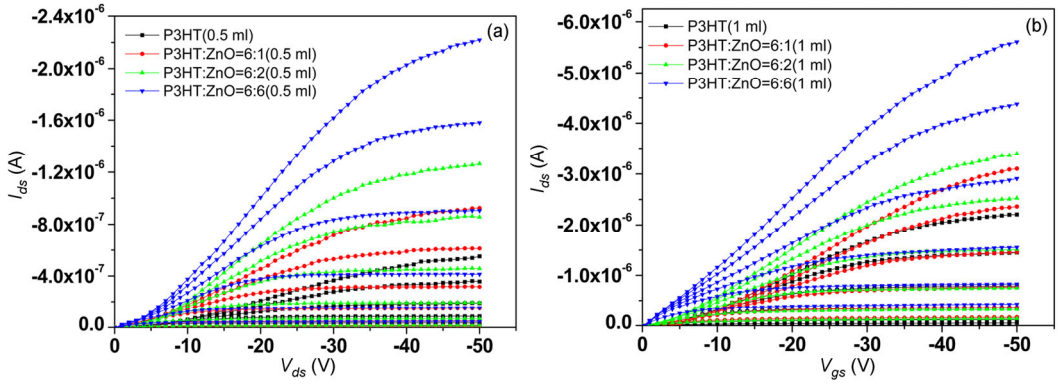

Figure 4 (Color online) The current-voltage (I_{ds} vs. V_{ds}) characteristics of OTFTs with gate bias voltage swept from 0 V to −50 V in a step of −10 V.

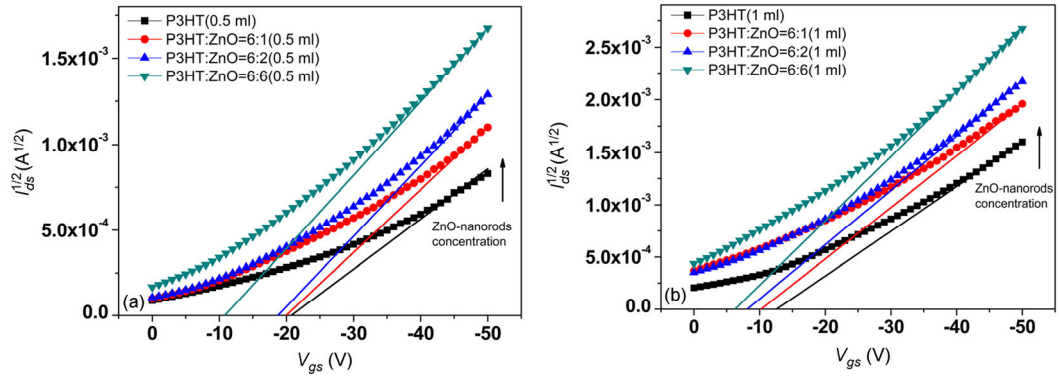

Figure 5 (Color online) The current-voltage (I_{ds} vs. V_{gs}) characteristics of OTFTs at the V_{ds} of −50 V.

P3HT was that more holes carriers were provided in the channel, which also contributed to the increase of μ. However, the thinner OTFT demonstrated good agreement with the expected OTFT electronic characteristics, i.e., I_{ds} varied linearly at low V_{ds} and saturated at higher V_{ds} for a fixed V_{gs}. The I_{on} increased with film thickness, but the I_{off} increased faster with film thickness. Therefore, lower I_{on}/I_{off} was observed for the thicker film as shown in Table 1.

3.4 The electronic characteristics of OTFTs with different concentration of ZnO-nanorods

As shown in Figure 6, the mobility of OTFTs prepared at spray volume of 0.5 mL increased with the ZnO-nanorods amount from 5.49×10^{-4} to 1.29×10^{-3} cm^2/Vs. Similarly, the mobility of OTFTs prepared at spray volume of 1 mL increased with the ZnO-nanorods amount from 1.30×10^{-3} to 2.62×10^{-3} cm^2/Vs. The mobility of composite film was as twice as that of the pristine P3HT film due to ZnO-nanorods doping. Comparing with the composite films of P3HT and TiO_2 nanorods, the increase of mobility caused by TiO_2 nanorods doping was about 80% [9]. To investigate this phenomenon, X-ray diffraction (XRD) measurements were carried out to characterize the P3HT thin films as a function of the ZnO-nanorods concentration. Figure 7 showed the

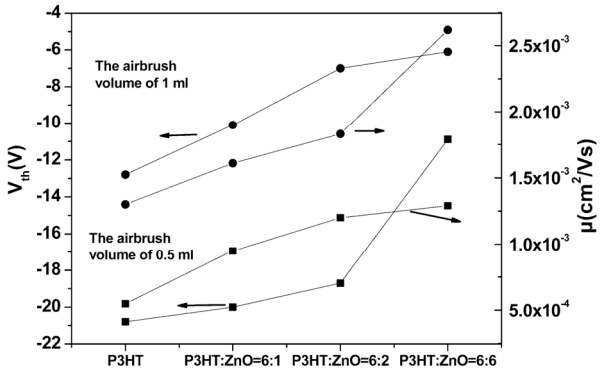

Figure 6 The mobility (μ) and threshold voltage (V_{th}) of OTFTs with ZnO-nanorod/P3HT composite films versus weight ratio of P3HT to ZnO-nanorod.

XRD spectra of three different weight ratio P3HT/ZnO-nanorods composite films with a pure P3HT film as control. The (100) peak can be observed in the pure P3HT film and the P3HT/ZnO-nanorods composite film. The peak intensity of the latter one was even higher than that of the former one, revealing that more plane-on P3HT domains were generated when it was mixed with ZnO-nanorods [27]. As the increase of ZnO-nanorods, the intensity of the (100) peak was significantly reduced. The dispersed ZnO-nanorods may dis-

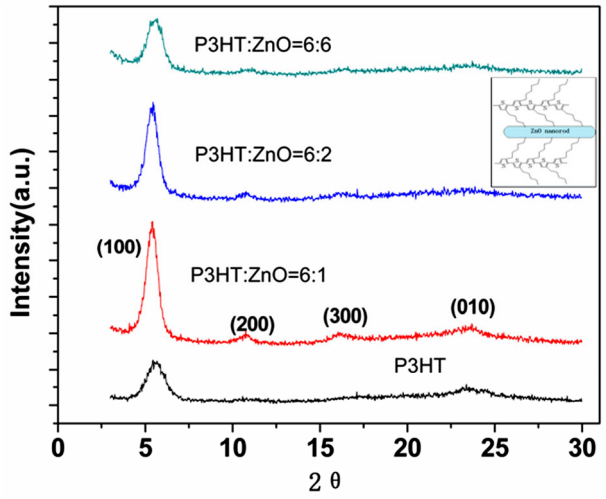

Figure 7 (Color online) Out-of-plane grazing-incidence angle X-ray diffraction intensities as a function of the scattering angle 2θ for P3HT thin films on SiO2/Si substrates with various ZnO-nanorod concentrations.

turb the molecular ordering of the P3HT film. However, the (010) peak cannot be observed in the composites regardless of the increase of ZnO-nanorods weight ratio and thus edge-on P3HT domains dominated in the composite films, which were favorable for carrier transfer in P3HT films. Therefore, the orientation of the P3HT chain was influenced by the ZnO-nanorods, which can be regarded as a reason why the ZnO-nanorods doping increased the mobility in P3HT films.

UV-visible absorption spectrum of the thin P3HT film and the P3HT/ZnO-nanorods composite film with different amount of ZnO-nanorods were presented in Figure 8. Typically, P3HT showed three absorption peaks in the visible region, in which the ones at about 560 nm and at about 524 nm was related to π to π^* transition [28]. The absorption shoulder at around 603 nm was associated with the interchain interaction and thus the height of this shoulder indicated the ordering of the chain packing [28, 29]. A red shift of the peak at ~520 nm was observed as well as a higher peak at ~603 nm compared with a pristine P3HT film, indicating the longer conjugation length and better π-π stacking of the P3HT chains in the composite film, respectively[9]. Therefore, the large enhancement in carrier mobility of the eight OTFTs may be attributable to the improvement of ordering in P3HT introduced by ZnO-nanorods doping.

Besides, the heterojunction formed by P3HT (p-type) and ZnO-nanorods (n-type). Since the work function of the P3HT was smaller than that of the ZnO-nanorods ($\varphi_p<\varphi_n$), the space-charge region consisted of the induced free charges on either side of the heterojunction [30]. The accumulation heterojunction was formed as shown in Figure 9. Electron injected into ZnO-nanorods from P3HT and $P3HT^+$ occured simultaneously. Therefore, the majority carriers were accumulated on either side of the P3HT-ZnO interface. As the concentration of ZnO-nanorods increased, the area of carriers accumulation enlarged, which benefited carrier transfer in OTFTs with P3HT films.

The V_{th} of OTFTs based on P3HT/ZnO-nanorods composite film was more positive than that of OTFTs based on pristine P3HT film due to the electrostatic potential change as shown in Figure 6. The threshold voltage V_{th} of a p-type OTFT is given by

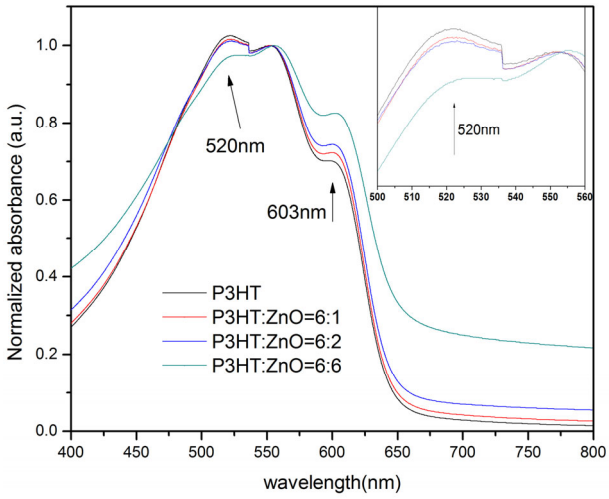

Figure 8 (Color online) UV-visible absorption spectra of P3HT and P3HT/ ZnO-nanorods composite films.

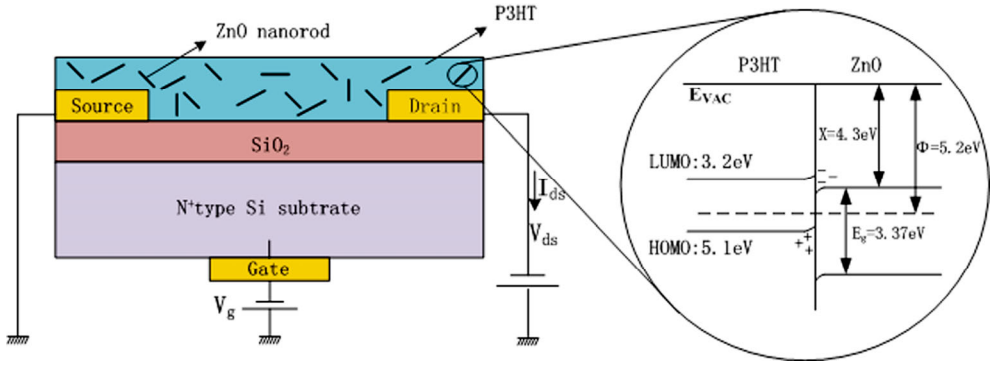

Figure 9 (Color online) Schematic of OTFT with ZnO-nanorod/P3HT composite films and energy level diagram of the interfaces between P3HT and ZnO-nanorod.

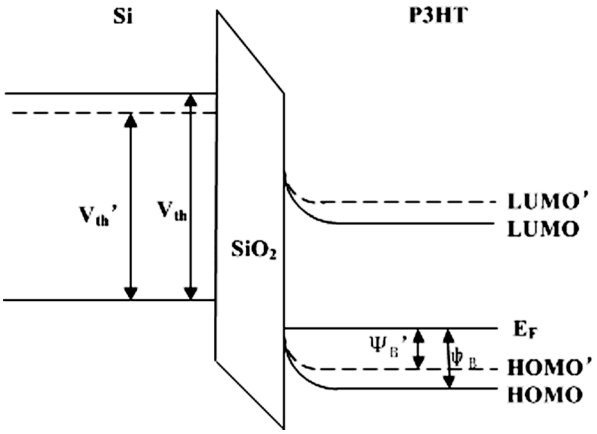

Figure 10 Energy-band diagrams for an OTFT under gate biases of its threshold voltage.

$$V_{th} = V_{FB} - \psi_B - \frac{\sqrt{2\varepsilon_S q N_D \psi_B}}{C_i}. \quad (4)$$

where ψ_B is the electrostatic potential in the active layer (ψ_B is also the potential difference between the HOMO and the Fermi level of the semiconducting polymer), N_D is the effective doping level of the organic semiconductor, ε_s is the dielectric constant of the semiconductor, C_i is the capacitance of the gate insulator per unit area, and V_{FB} is the flat-band voltage of the device. The electrostatic potential of the active layer P3HT/ZnO-nanorods composite film would decrease as a result of electrons accumulated in the ZnO-nanorods and thus change the threshold voltage of the device, as shown in Figure 10 [11]. Therefore, the threshold voltage V_{th} will change positively with a decrease in ψ_B.

4 Conclusion

OTFT employing pristine P3HT film and P3HT/ZnO-nanorods composite film as active layers were fabricated by spray-coating technology. The value of V_{th} was observed to become more positive as the P3HT thickness increased. Meanwhile, the mobility and I_{ds} increased with the thickness. The reason was that more hole carriers owing to higher surface potential at the interface of P3HT/SiO_2 for thicker film were supplied in channel. Furthermore, the remarkable increase of the field-effect mobility over that of the pristine P3HT film was due to the ZnO-nanorods doping. ZnO-nanorods improved the crystallinity of P3HT, optimized orientation of polymer chains and formed the heterojunction in the composite films. In addition, the threshold voltage was changed because the electronic potential decreased which was attributed to electrons accumulated in the ZnO-nanorods. The results indicate that the electrical properties of P3HT film were improved by introducing ZnO-nanorods into film, although the performance of prepared OTFT was low in some aspects, which were of general importance for their application in solar cells, transistors, or other semiconductor devices.

This work is partially supported by the foundation for Innovation Research Groups of the National Natural Science Foundation of China (NSFC) (Grant No.61421002), the National Natural Science Foundation of China (Grant Nos. 61571097).

1 Wu S, Tai Q, Yan F. Hybrid photovoltaic devices based on poly (3-hexylthiophene) and ordered electrospun ZnO nanofibers. J Phys ChemC, 2010, 114: 6197–6200
2 Coakley K M, Srinivasan B S, Ziebarth J M, et al. Enhanced hole mobility in regioregular polythiophene infiltrated in straight nanopores. Adv Funct Mater, 2005, 15: 1927–1932
3 Unalan H E, Hiralal P, Kuo D, et al. Flexible organic photovoltaics from zinc oxide nanowires grown on transparent and conducting single walled carbon nanotube thin films. J Mater Chem, 2008, 18: 5909
4 Wu M-C, Lin Y-Y, Chen S, et al. Enhancing light absorption and carrier transport of P3HT by doping multi-wall carbon nanotubes. Chem Phys Lett, 2009, 468: 64–68
5 Tai Q, Zhao X, Yan F. Hybrid solar cells based on poly(3-hexylthiophene) and electrospun TiO_2 nanofibers with effective interface modification. J Mater Chem, 2010, 20: 7366
6 Bouclé J, Chyla S, Shaffer M S P, et al. Hybrid solar cells from a blend of Poly(3-hexylthiophene) and ligand-capped TiO_2 nanorods. Adv Funct Mater, 2008, 18: 622–633
7 Lin Y-Y, Chu T-H, Li S-S, et al. Interfacial nanostructuring on the performance of polymer/TiO_2 nanorod bulk heterojunction Solar cells. J AM Chem Soc, 2009, 3644–3649
8 Yang Y, Guo W, Zhang Y, et al. Piezotronic effect on the output voltage of P3HT/ZnO micro/nanowire heterojunction solar cells. Nano Lett, 2011, 11: 4812–4817
9 Sun Z, Li J, Liu C, et al. Enhancement of hole mobility of poly(3-hexylthiophene) induced by titania nanorods in composite films. AdvMater, 2011, 23: 3648–3652
10 Park Y D, Lim J A, Jang Y, et al. Enhancement of the field-effect mobility of poly(3-hexylthiophene)/functionalized carbon nanotube hybrid transistors. Org Electron, 2008, 9: 317–322
11 Yan F, Li J, Mok S M. Highly photosensitive thin film transistors based on a composite of poly(3-hexylthiophene) and titania nanoparticles. J Appl Phys, 2009, 106: 074501
12 Kim S, Kwon H-J, Lee S, et al. Low-power flexible organic light-emitting diode display device. AdvMater, 2011, 23: 3511–3516
13 Rotzoll R, Mohapatra S, Olariu V, et al. Radio frequency rectifiers based on organic thin-film transistors. Appl Phys Lett, 2006, 88: 123502
14 Li B, Lambeth D N. Chemical sensing using nanostructured polythiophene transistors. Nano Lett, 2008, 8: 3563–3567
15 Das A, Dost R, Richardson T, et al. A Nitrogen Dioxide Sensor Based on an Organic Transistor Constructed from Amorphous Semiconducting Polymers. Adv Mater, 2007, 19: 4018–4023
16 Deng J, Wang M, Song X, et al. CdS and CdSe quantum dots subsectionally sensitized solar cells using a novel double-layer ZnO nanorod arrays. J Colloid Interface Sci, 2012, 388: 118–122
17 Shen Q, Ogomi Y, Das S K, et al. Huge suppression of charge recombination in P3HT-ZnO organic-inorganic hybrid solar cells by locating dyes at the ZnO/P3HT interfaces. Phys Chem Chem Phys, 2013, 15: 14370–14376
18 Noori K, Giustino F. Ideal energy-level alignment at the ZnO/P3HT photovoltaic interface. Adv Funct Mater, 2012, 22: 5089–5095
19 Kang D, Liu a, Bian J, et al. Optoelectronic characteristics of Zinc oxide nanorods/P3HT hybrid junctions investigated using surface photovoltage method. ECS Solid State Letters, 2012, 1: 15–17
20 Li F, Chen W, Yuan K, et al. Photovoltaic performance enhancement

in P3HT/ZnO hybrid bulk-heterojunction solar cells induced by semiconducting liquid crystal ligands. Org Electron, 2012, 13: 2757–2762
21 Mok S M, Yan F, Chan H L W. Organic phototransistor based on poly(3-hexylthiophene)/TiO[sub2] nanoparticle composite. Appl Phys Lett, 2008, 93: 023310
22 Xie T, Xie G, Zhou Y, et al. Thin film transistors gas sensors based on reduced graphene oxide poly(3-hexylthiophene) bilayer film for nitrogen dioxide detection. Chem. Phys. Lett. 2014, 614: 275–281
23 Wang L, Kang Y, Liu X, et al. ZnO nanorod gas sensor for ethanol detection. Sensors Actuators B: Chem, 2012, 162: 237–243
24 von Hauff E, Johnen F, Tunc A V, et al. Detailed investigation of the conducting channel in poly(3-hexylthiophene) field effect transistors. J Appl Phys, 2010, 108: 063709
25 Chabinyc M L, Lu J-P, Street R A, et al. Short channel effects in regioregular poly(thiophene) thin film transistors. J Appl Phys, 2004, 96: 2063
26 Jia H, Gowrisanker S, Pant G K, et al. Effect of poly (3-hexylthiophene) film thickness on organic thin film transistor properties. J Vac Sci Technol A, 2006, 24: 1228
27 Sirringhaus H, Brown P J, Friend R H, et al. Two-dimensional charge transport in conjugated polymers. Nature, 1999, 401: 685–688
28 Brown P, Thomas D, Köhler A, et al. Effect of interchain interactions on the absorption and emission of poly(3-hexylthiophene). Phys Rev B, 2003, 67: 064203
29 Brown P, Sirringhaus H, Harrison M, et al. Optical spectroscopy of field-induced charge in self-organized high mobility poly(3-hexylthiophene). Phys Rev B, 2001, 63: 125204
30 Wang H, Yan D. Organic heterostructures in organic field-effect transistors. Asia Mater, 2010, 2: 69–78